TU Delft

Delft University of Technology

Effect of partial coherent illumination on Fourier Ptychography

Heemels, Alex; Agbana, Tope; Pereira, Silvania; Diehl, Jan-Carel; Verhaegen, Michel; Vdovin, Gleb

DOI
10.1117/12.2544766

Publication date
2020

Document Version
Final published version

Published in
Proceedings of SPIE

Citation (APA)
Heemels, A., Agbana, T., Pereira, S., Diehl, J.-C., Verhaegen, M., & Vdovin, G. (2020). Effect of partial coherent illumination on Fourier Ptychography. In N. T. Shaked, & O. Hayden (Eds.), *Proceedings of SPIE: Label-Free Biomedical Imaging and Sensing (LBIS) 2020* (Vol. 11251). Article 112511K (Progress in Biomedical Optics and Imaging - Proceedings of SPIE; Vol. 11251). SPIE.
https://doi.org/10.1117/12.2544766

Important note
To cite this publication, please use the final published version (if applicable).
Please check the document version above.

Copyright
Other than for strictly personal use, it is not permitted to download, forward or distribute the text or part of it, without the consent of the author(s) and/or copyright holder(s), unless the work is under an open content license such as Creative Commons.

Takedown policy
Please contact us and provide details if you believe this document breaches copyrights.
We will remove access to the work immediately and investigate your claim.

This work is downloaded from Delft University of Technology.
For technical reasons the number of authors shown on this cover page is limited to a maximum of 10.

PROCEEDINGS OF SPIE

SPIEDigitalLibrary.org/conference-proceedings-of-spie

Effect of partial coherent illumination on Fourier Ptychography

Heemels, Alexander, Agbana, Temitope, Pereira, Silvania, Diehl, Jan Carel, Verhaegen, Michel, et al.

Alexander Heemels, Temitope Agbana, Silvania Pereira, Jan Carel Diehl, Michel Verhaegen, Gleb Vdovin, "Effect of partial coherent illumination on Fourier Ptychography," Proc. SPIE 11251, Label-free Biomedical Imaging and Sensing (LBIS) 2020, 112511K (20 February 2020); doi: 10.1117/12.2544766

SPIE.

Event: SPIE BiOS, 2020, San Francisco, California, United States

Downloaded From: https://www.spiedigitallibrary.org/conference-proceedings-of-spie on 06 Mar 2020 Terms of Use: https://www.spiedigitallibrary.org/terms-of-use

Effect of partial coherent illumination on Fourier Ptychography

Alexander Heemels[a,b], Temitope Agbana[a], Silvania Pereira[b], Jan Carel Diehl[c], Michel Verhaegen[a], and Gleb Vdovin[a]

[a]Delft University of Technology, Delft Center for System and Control, Delft, Netherlands
[b]Delft University of Technology, Department of Imaging Physics, Delft, Netherlands
[c]Delft University of Technology, Industrial Design Engineering, Delft, Netherlands

ABSTRACT

Fourier Ptychography is a computational imaging technique able to decouple high resolution from wide field of view, bypassing the diffraction limit of the microscope. Since it does not rely on high precision mechanics or fluorescent imaging, it is of practical interest for implementation in low scale devices. Despite its gains, realizing a functional low-cost setup working at the theoretical limits is challenging due to many factors causing discrepancies between theory and practice. Misalignment of the light emitting diode array (LED-array), optical system aberrations and use of partial coherent sources are common issues which have been addressed with calibration algorithms. However, physical interpretation of how these factors influence the algorithm and cause mismatches between theory and practice has had little attention so far. This work provides a discussion based on simulation results on the effect of the partial coherence of the source. From obtained results, an optimal set of LEDs for data acquisition is described which avoids degeneracy caused by partial coherence and is based on the numerical aperture (NA) of the objective and source parameters such as bandwidth and size.

Keywords: Fourier Ptychography, Partial Coherence, Coherence, Physical Optics

1. INTRODUCTION

Fourier Ptychography[1] is based on developments in synthetic aperture techniques[2] and phase retrieval algorithms.[3,4] It is able to increase the space bandwidth product (SBP) of the microscope by combining angular illumination variation and computational techniques. It is based on coherent imaging, allowing images to be expressed as a convolution operation of the object with the impulse response of the optical system.[5] However, this assumption does not fully apply when imaging with a Light Emitting Diodes (LEDs). LEDs have low spatial and temporal coherence which implies that image formation is better described by a partial coherent model. As light from a partial coherent source gains coherence is through propagation[6] the Van Cittert Zernike Theorem[7] can be used to determine a coherent area with radius R_{coh} based on the distance from source to sample h_s, the radial size of the source ρ_s and its mean wavelength $\bar{\lambda}$:

$$R_{coh} = \frac{0.16\bar{\lambda}h_s}{\rho_s} \tag{1}$$

Thus, increasing the source-sample distance results in a larger area that can be assumed to be coherent and allows coherent image reconstruction if the reconstructed image size is contained within the coherent area.

However, Fourier Ptychography is mostly used in low NA systems with low magnification and imaging sensor with over millions of pixels. In this case coherent reconstruction of the full field of view implies the reconstruction of several hundreds of these coherent areas, making it time inefficient. In this work, we analyse the impact of partial coherence and the extent to which reconstruction with image sizes exceeding the coherent area can be done without any significant degradation in reconstruction quality. This is done by adapting the image formation model to allow generation of partially coherent images with varying temporal and spatial coherence. After which, the effect on the reconstructed object is analyzed and a solution for mitigating the negative influences is provided.

Further author information: (Send correspondence to)
Alexander Heemels: E-mail: A.N.M.Heemels@tudelft.nl, Telephone: +31 152785305
Temitope E. Agbana: E-mail: T.E.Agbana@tudelft.nl, Telephone: +31 152785305

Label-free Biomedical Imaging and Sensing (LBIS) 2020, edited by Natan T. Shaked, Oliver Hayden, Proc. of SPIE Vol. 11251, 112511K · © 2020 SPIE
CCC code: 1605-7422/20/$21 · doi: 10.1117/12.2544766

Downloaded From: https://www.spiedigitallibrary.org/conference-proceedings-of-spie on 06 Mar 2020
Terms of Use: https://www.spiedigitallibrary.org/terms-of-use

2. MODEL MODIFICATIONS

To allow generation of partial coherent images the image formation model is adapted by decomposing the partial coherent source into mutual coherent modes.[8,9] As such, the image of the partial coherent system can be modelled as an incoherent summation of the images produced by the coherent modes of the source:

$$I_i = \sum_{l}^{L} \sum_{m}^{M} |I_{i,m,l}(\mathbf{r})|^2 \tag{2}$$

With i denoting the index of the illumination LED, m the m-th spatial modes of the extended light source and l the l-th spectral mode of the emitting bandwidth. In simulations this is implemented by dividing each LED into M monochromatic point sources bound to the light emitting surface of the LEDs and L monochromatic point sources corresponding to different emission wavelengths of the LEDs bandwidth. The distribution of these modes is best observed in the k-space of the LED-array (Fig. 1).

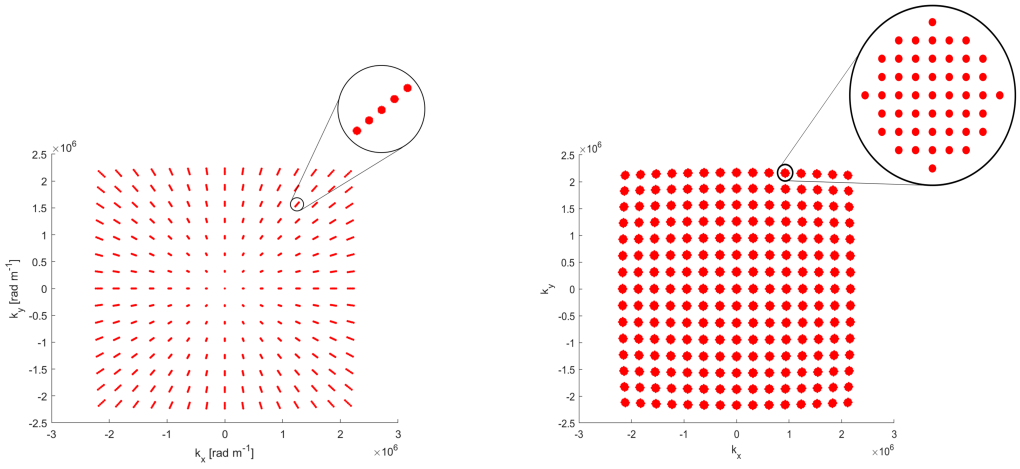

(a) (b)

Figure 1: (a) K-space distribution of the LED-arrays temporal modes; (b) K-space distribution of the LED-arrays spatial modes

3. SIMULATIONS AND RESULTS

Simulations make use of 3 sets of 2 images making up the amplitude and phase of the simulated objects (Fig. 2). This is done to compare global trends in convergence behavior and exclude image dependent behavior *.
An offset invariant Root Mean Squared Error (RMSE) metric is used to track the error $\mathcal{E}_k$ between reconstruction $\tilde{X}_k$ at iteration k with the original object X.[10]

$$\mathcal{E}_k = \frac{||\mathcal{F}(X) - \alpha\mathcal{F}(\tilde{X}_k)||_2^2}{||\mathcal{F}(X)||_2^2} \tag{3}$$

$$\alpha = \frac{\mathcal{F}(X)\mathcal{F}(\tilde{X}_k)^*}{|\mathcal{F}(\tilde{X}_k)|^2} \tag{4}$$

Spatial and spectral modes are analyzed separately for the cases of 81 and 441 images; this allows for analysis on only bright field reconstruction and identify potential issues caused by the inclusion of dark field images.

*All images were obtained from http://imagecompression.info/test_images/

Downloaded From: https://www.spiedigitallibrary.org/conference-proceedings-of-spie on 06 Mar 2020
Terms of Use: https://www.spiedigitallibrary.org/terms-of-use

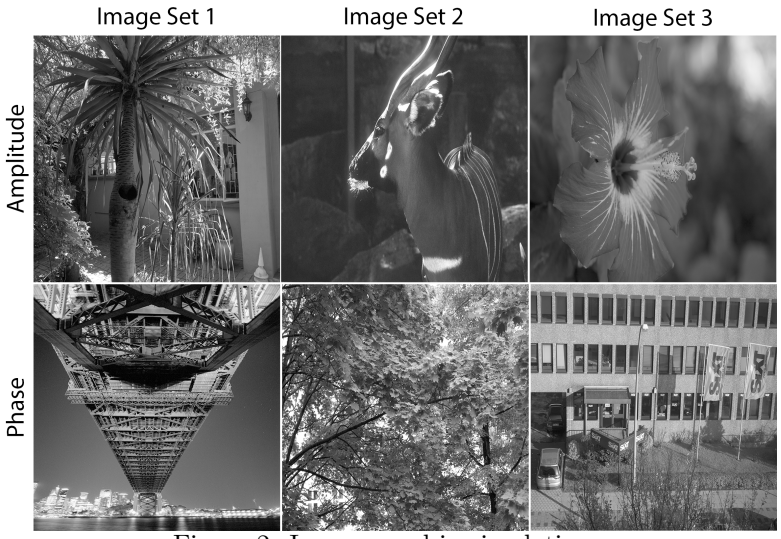

Figure 2: Images used in simulations

By varying the size of the source from 0-500μm, the area which can be assumed coherent in the sample plane decreases. Once the source size exceeds 330μm, the reconstruction can no longer be assumed coherent according to Eq. 1. This is confirmed by the simulation results using 81 images (Fig. 3a) as once the threshold of 330μm is passed an increase in RMSE is observed (Fig. 3b). For increasing bandwidths $\Delta\lambda$ =0-100nm, no major increases in RMSE are observed (Fig. 3c).

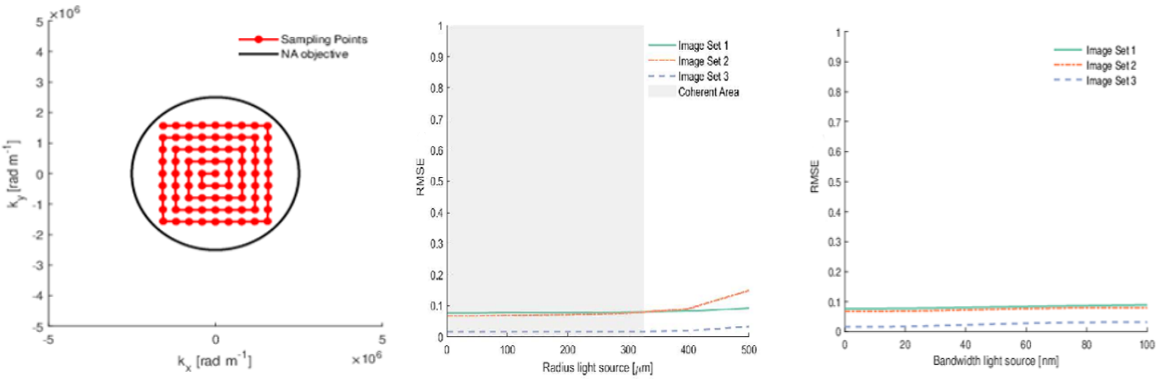

(a) (b) (c)

Figure 3: (a) Sampling sequence for 81 images used for all 3 image sets; (b) Final root mean square errors for 81 images with the radii of the source varying from 0-500μm; (c) Final root mean square errors for 81 images with the LED's bandwidth varying from 0-100nm.

Increasing the number of images to 441 (Fig. 4a) and including the darkfield images causes large increases in error within the coherent area (Fig. 4b) and massive jumps in the spectral error at small bandwidths (Fig.4c).

Downloaded From: https://www.spiedigitallibrary.org/conference-proceedings-of-spie on 06 Mar 2020
Terms of Use: https://www.spiedigitallibrary.org/terms-of-use

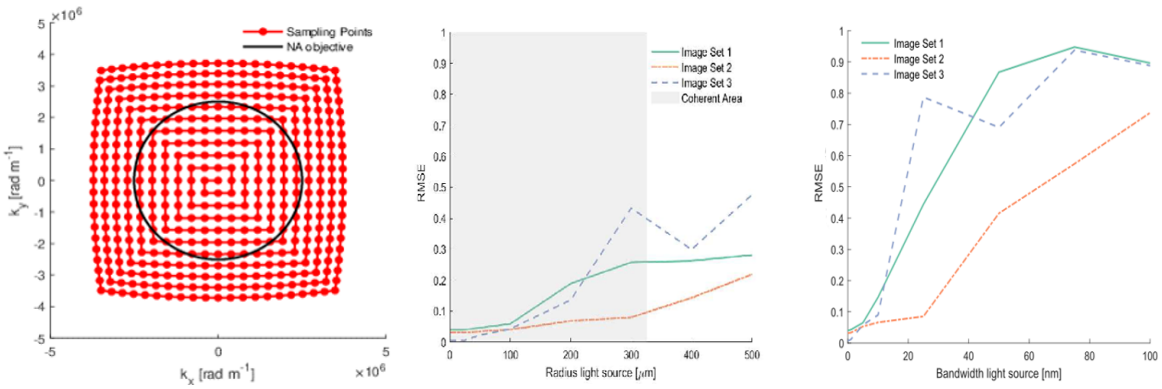

(a) (b) (c)

Figure 4: (a) Sampling sequence for 441 images; (b) Final root mean square errors for 441 images and all 3 image sets with the radii of the source bandwidth varying from 0-100nm; (c) Final root mean square errors for 441 images and all 3 image sets with the radii of the source varying from 0-500μm

The cause of these errors are identified by tracking the RMSE at the end of each image update step in the Fourier Ptychographic algorithm and identifying the images of LEDs which increase the RMSE. An overview of LEDs (in k-space) which increase/decrease the RMSE are shown in Fig. 5. Notice that LEDs with a negative contribution have k-values close numerical aperture of the objective, suggesting that these are most sensitive to the effects of the spatial modes.

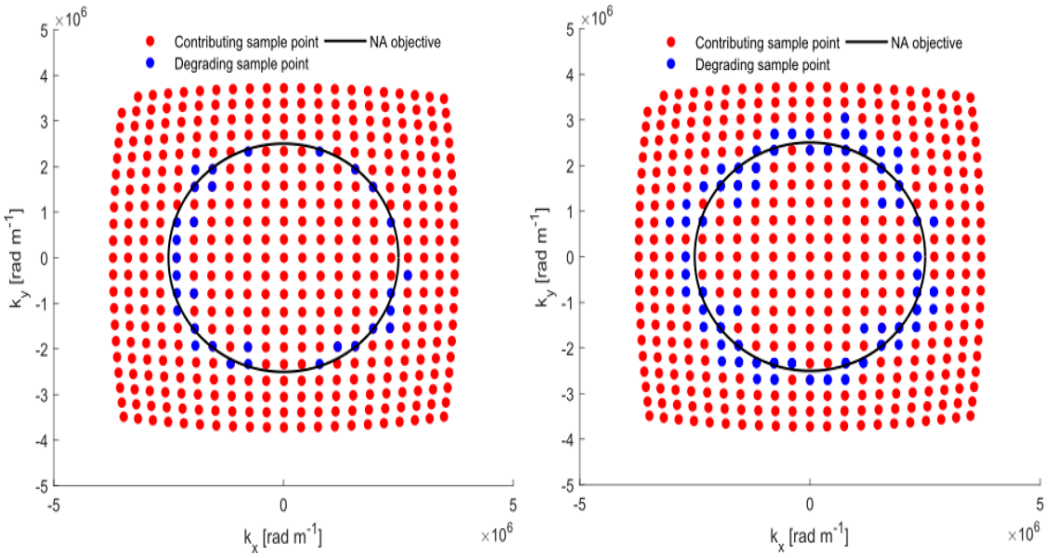

(a) (b)

Figure 5: Visualization of LEDs with positive contribution (red) and negative contribution (blue) (a) Reconstruction for spatial modes, source size 500μm; (b) Spectral modes $\Delta\lambda = 100$nm

This increase in RMSE is caused by spatial or spectral modes falling both in- and outside the NA boundary, causing these images to be a summation of both bright-and dark field images. Because the two types of images have different energy contents, this causes a decrease/increase in the total energy of the composite image - compared to the ideal coherent case- and in turn introduces errors into the reconstructed object.
By removing these LEDs such as in (Fig. 6), the reconstruction errors decrease drastically, as shown in Fig. 7.

Downloaded From: https://www.spiedigitallibrary.org/conference-proceedings-of-spie on 06 Mar 2020
Terms of Use: https://www.spiedigitallibrary.org/terms-of-use

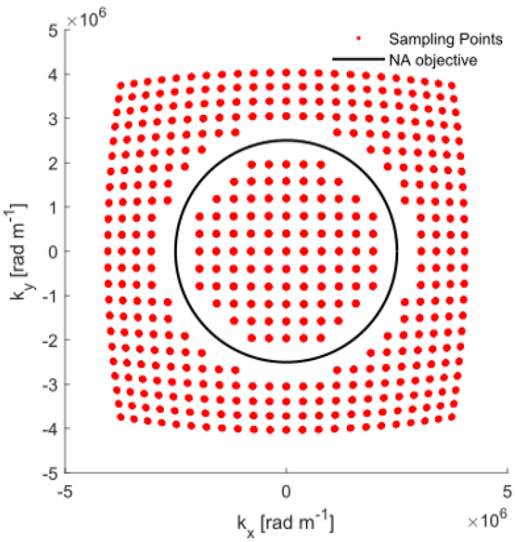

Figure 6: Sampling scenario with spatial modes, with LEDs close to the NA circle left out, avoiding spatial modes falling both in and outside of the NA circle

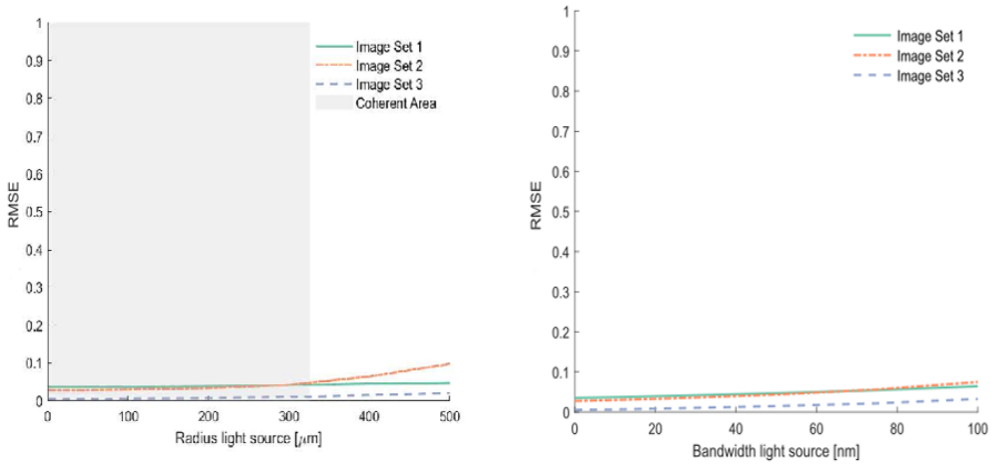

(a) (b)

Figure 7: (a) Final convergence errors for new sampling sequence (Fig. 6) and all 3 image sets with the radii of the source varying from 0-500μm: Final spectrum convergence values; (b) Final convergence errors for new sampling sequence (Fig. 6) and all 3 image sets with the radii of the source bandwidth varying from 0-100nm: Final spectrum convergence value

Visual inspection of the reconstruction results for bandwidths of 10, 50 and 100nm shows the degrading effects when the boundary LEDs are included into the reconstruction (Fig. 8). When these LEDs are excluded, the reconstruction improves greatly, with deterioration only attributed to the increase in bandwidth (Fig.9).

Downloaded From: https://www.spiedigitallibrary.org/conference-proceedings-of-spie on 06 Mar 2020
Terms of Use: https://www.spiedigitallibrary.org/terms-of-use

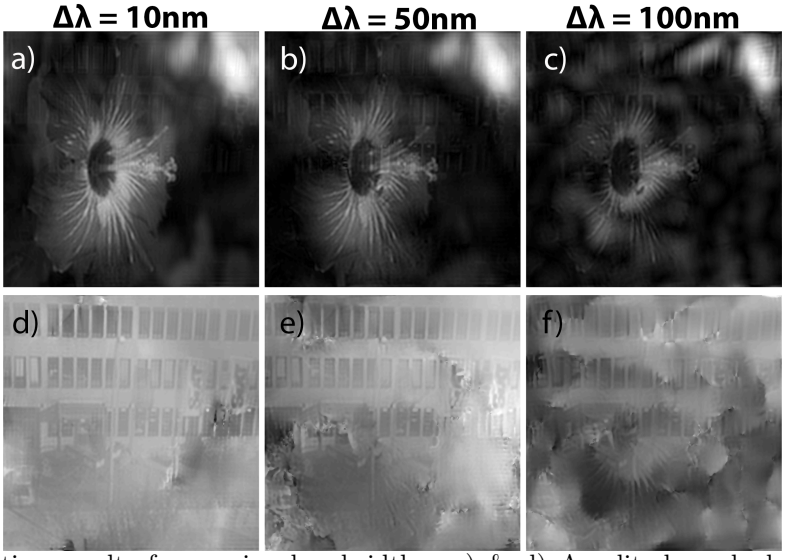

Figure 8: Reconstruction results for varying bandwidths: a) & d) Amplitude and phase reconstruction for $\Delta\lambda = 10$nm; b) & e) Amplitude and phase reconstruction for $\Delta\lambda = 50$nm; c) & f) Amplitude and phase reconstruction for $\Delta\lambda = 100$nm

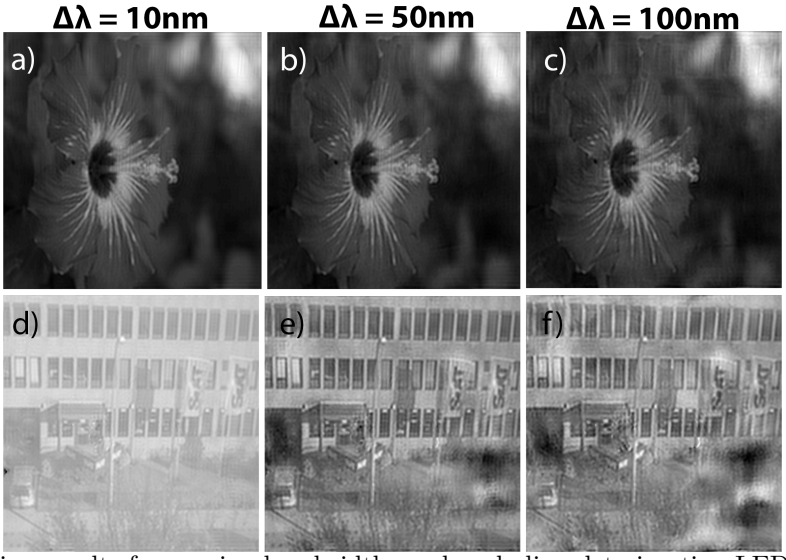

Figure 9: Reconstruction results for varying bandwidths and excluding deteriorating LEDs: a) & d) Amplitude and phase reconstruction for $\Delta\lambda = 10$nm; b) & e) Amplitude and phase reconstruction for $\Delta\lambda = 50$nm; c) & f) Amplitude and phase reconstruction for $\Delta\lambda = 100$nm

It is possible to formulate a closed form expression of an exclusion band $\mathcal{B}$, depending on the spread of the spatial coherent modes r_ρ:

$$r_\rho = k_0 \frac{\rho_s}{\sqrt{\rho_s^2 + h_{LED}^2}} \tag{5}$$

And the spread of the spectral coherent modes r_λ

$$r_\lambda = \Delta_\lambda \nabla_\lambda \tag{6}$$

Downloaded From: https://www.spiedigitallibrary.org/conference-proceedings-of-spie on 06 Mar 2020
Terms of Use: https://www.spiedigitallibrary.org/terms-of-use

With $\nabla_{\lambda,i}$ the gradient of the LEDs position in k-space with respect to the wavelength.

$$\nabla_{\lambda,i} = \frac{\partial \mathbf{k}_i}{\partial \lambda} = -\frac{k}{2\pi}\mathbf{k}_i$$

The exclusion bound is then denoted by:

$$\mathcal{B} = k_0 \mathrm{NA}_{obj} \pm \max(r_\lambda \nabla_\lambda + r_\rho) \tag{7}$$

4. CONCLUSIONS

Using simulation studies, it has been shown that the LEDs with illumination angles close to the numerical aperture of the objective lens are sensitive to the effects of partial coherence. This sensitivity is caused by the spatial and spectral modes of the light source falling both in- and outside the NA of the objective, causing energy mismatches in the composite partial coherent image compared to the expected coherent case.
These degrading effects can be mitigated by removing LEDs within an exclusion boundary depending on the properties of the source.

REFERENCES

[1] Zheng, G., Horstmeyer, R., and Yang, C., "Wide-field, high-resolution Fourier ptychographic microscopy," *Nature Photonics* **7**(9), 739–745 (2013).

[2] Turpin, T. M., Gesell, L. H., Lapides, J., and Price, C. H., "Theory of the synthetic aperture microscope," (August 1995), 230–240 (1995).

[3] Fienup, J. R., "Phase retrieval algorithms: a comparison," *Applied Optics* **21**(15), 2758 (1982).

[4] Shechtman, Y., Eldar, Y. C., Cohen, O., Chapman, H. N., Miao, J., and Segev, M., "Phase Retrieval with Application to Optical Imaging: A contemporary overview," *IEEE Signal Processing Magazine* **32**(3), 87–109 (2015).

[5] Goodman, J. W., "Introduction to Fourier Optics McGraw-Hill Series in Electrical and Computer Engineering," *Quantum and Semiclassical Optics Journal of the European Optical Society Part B* **8**(5), 491 (1996).

[6] Brady, D. J., [*Optical Imaging and Spectroscopy*], John Wiley & Sons, Inc., Hoboken, NJ, USA (mar 2008).

[7] Born, M., Wolf, E., Bhatia, A. B., Clemmow, P. C., Gabor, D., Stokes, A. R., Taylor, A. M., Wayman, P. A., and Wilcock, W. L., [*Principles of Optics*] (1999).

[8] Wolf, E., "New theory of partial coherence in the space-frequency domain Part I: Steady-state fields and higher-order correlations," *Journal of the Optical Society of America A* **3**(1), 76 (1986).

[9] Thibault, P. and Guizar-Sicairos, M., "Maximum-likelihood refinement for coherent diffractive imaging," *New Journal of Physics* **14** (2012).

[10] Fienup, J. R., "Invariant error metrics for image reconstruction," *Applied Optics* **36**(32), 8352 (1997).

Downloaded From: https://www.spiedigitallibrary.org/conference-proceedings-of-spie on 06 Mar 2020
Terms of Use: https://www.spiedigitallibrary.org/terms-of-use